forests

MDPI

Article

Droughts Are Not the Likely Primary Cause for *Abies sibirica* and *Pinus sibirica* Forest Dieback in the South Siberian Mountains

Nadezhda M. Tchebakova [1,*], Elena I. Parfenova [1], Elena V. Bazhina [1], Amber J. Soja [2] and Pavel Ya. Groisman [3]

1 Sukachev Forest Institute of FRC KSC SB RAS, Academgorodok, 50/28, 660036 Krasnoyarsk, Russia
2 National Institute for Aerospace, NASA Langley Research Center, Hampton, VA 23681, USA
3 North Carolina State University at NOAA National Center for Environmental Information, Asheville, NC 28801, USA
* Correspondence: ncheby@ksc.krasn.ru

Abstract: *Background*. Since the mid-20th century, massive dieback of coniferous forests has been observed in the temperate and boreal zones across North America and Northern Eurasia. The first hypotheses explaining forest dieback were associated with industrial air pollution (acid rain). At the end of the century, new hypotheses emerged that supported critical climate-induced aridization to explain forest dieback. Many studies were based on the SPEI (Standardized Precipitation Evapotranspiration Index) drought index. Our goals were to investigate if the SPEI drought index was a suitable metric to reflect drought conditions in wet and moist dark-needled forests in the South Siberian Mountains (Mts) and if droughts trigger the dieback of those forests. *Methods.* We calculated the SPEI drought index, the annual moisture index AMI, potential evapotranspiration PET, and water balance dynamics for the period 1961–2019 for four transects in the South Siberian Mts. where decline/dieback of dark-needled Siberian pine and fir forests were identified *in situ*. Climate data from nine weather stations located at lower and upper elevations of each transect were used to calculate climatic index dynamics for the 1961–2019 period to identify dry and wet phases of the period. *Results.* Our findings showed that climatic moisture/dryness indices have rarely gone down to high risk levels during the last 60 years (1961–2019). AMI did not reach the critical limit, 2.25, characteristic of the lower border for the dark-needled taiga. SPEI values < -1.5 represent drought stress conditions for dark-needled conifers at the lower border, and these conditions occurred 3–4 times during the 60-year period. However, the annual water balance stayed positive in those years in wet and moist forests at mid-to-high elevations. Trees are known to survive occasional (1–2) dry years. We found that dark-needled conifer dieback often occurs in wet years with plentiful rain rather than in drought years. We found forest dieback was associated with the westerlies that bring atmospheric pollution from the west at 50–56 N latitudes, where the air masses cross populated regions that have widespread industrial complexes. *Conclusions*. We concluded that the observed decline of dark-needled conifers at middle-to-high elevations across the South Siberia's Mts was conditioned by several plausible causes, among which air pollution seems to be more credible, rather than dry climatic conditions, as cited in recent literature. Results are essential for understanding these ecosystems and others as our planet changes. Other causes and mechanisms should be further investigated, which would necessitate creating infrastructure that supports multi-disciplinary, inter-agency teamwork of plant physiologists, foresters, chemists, etc.

Keywords: boreal dark-needled forests; drought index SPEI; annual moisture index AMI; damaged stands; precipitation; potential evapotranspiration

Citation: Tchebakova, N.M.; Parfenova, E.I.; Bazhina, E.V.; Soja, A.J.; Groisman, P.Y. Droughts Are Not the Likely Primary Cause for *Abies sibirica* and *Pinus sibirica* Forest Dieback in the South Siberian Mountains. *Forests* **2022**, *13*, 1378. https://doi.org/10.3390/f13091378

Academic Editor: Stefan Arndt

Received: 12 August 2022
Accepted: 26 August 2022
Published: 29 August 2022

1. Introduction

Coniferous forests are the major renewable resource in Siberia. The forests in the South Siberian Mountains have been affected by excessive exploitation in recent decades; 80% of these forests have been logged [1,2]. The most valuable tree in these forests is the unique Siberian pine (*Pinus sibirica* Du Tour), called "cedar" in Russia, occupying 30% of the forested area across these mountains. Secondary forests composed of hardwoods currently replace conifer forests after intensive clear-cutting. In southern Siberia as a whole, models have shown that forest habitats would decrease by 30–40%, and in the southern Siberia montane foothills, these forests would be replaced by mixed light-needled and hardwood subtaiga. In a warmer climate, dark-needled forests would move upslope, replacing the tundra highlands by the end of the 21st century [3,4].

Foresters and ecologists register worldwide dieback of conifers across the boreal zone [5–18]. Since the 1970s, the decrease in conifers has become crucial in the South Siberian Mountains, which are the most productive and biodiverse dark-needled coniferous forests from the Holocene [16,19–29].

Mountains are excellent paragons for monitoring and modeling climate change effects on vegetation and forests because ecosystems, soils, and other biologic features sharply change with the drastic changes in temperature and precipitation along elevation gradients [30,31].

Scientists have observed the damage and decline of the dark-needled coniferous forests at mid-to-high elevations in the South Siberian Mountain range. The damage has been defined by: necroses of branches with generative organs causing microsporogenesis irregularities and low pollen vitality, chloroses, necroses, and premature needle falls [23,24,26]; the occurrence of stem rot in dark-needled trees [32]; and linear and radial growth increment decreases [14–16].

Currently, researchers suggest several *hypotheses* to explain the decline and dieback of dark-needled coniferous forests within 50–56° N latitudes across Northern Eurasia. These processes can be associated with four possible hypotheses:

- Climate aridization under global warming [9,16,33,34];
- Anthropogenic environmental pollution, which could include acid rain and/or the deposition of mercury, lead, zinc, cadmium, or other toxins [29,34–38];
- Phytopathogen (*Armillaria mellea, Heterobasidion annosum*, etc.) [39–41] and invasive insect pests [42,43]. Foresters and ecologists are generally skeptical that disease and infestations are the primary cause of forest death and decline, rather these are considered post-effects on previously weakened trees; and
- Increased ultraviolet (UV) radiation, as a result of stratosphere ozone depletion, amplified by the increased ozone concentration near the surface, and dimming [44–52].

Montane dark-needled forests across the South Siberian Mountains have been slowly decimated over the last several decades, from about 1961 through 2019. From the late 1990s to the mid-2000s, the dark-needled forest dieback became catastrophic at middle-elevation vegetation belts. Catastrophic damage by biotic agents (phytopathogen and infestations) has become prevalent because trees have been weakened by multiyear primary stress factors such as climate, air pollution, and increased ultraviolet radiation.

Siberian pine and fir forest health across the South Siberian Mountains have been well studied long before insect and pathogen outbreaks first occurred, and the forests started to transition from healthy, undamaged to severely damaged ecosystems. The level of damage in these unique ecosystems varied depending on elevation, slope, and aspect, and the most severely damaged forest stands were primarily located at middle (680–930 m) and high (1100–1450 m) elevations [19,22,23,26,27]. These altitudinal vegetation belts located on western and northern windward slopes received more precipitation in comparison to leeward slopes and were called "wet" or "excessively wet" [1].

Our goal was to investigate the reasons for the significant diebacks observed in moist dark-needled *Pinus sibirica Du Tour* and *Abies sibirica L.* forests at the mid-to-highlands across the well-studied South Siberian Mountains. Our motivation was our initial research, conducted over the last several decades, which we believed often diverged from droughts driving the dieback, based on near-field meteorological and field data that was often contrary to drought. Another goal was to test the suitability of the SPEI drought index, as a metric with which to ascertain drought conditions in moist mid-to-highlands of the mountains (hypothesis #1).

Consequently, we integrated the data to accept/reject hypothesis and elucidate suppositions:

1. Climate at mid-to-higher elevations across the South Siberia Mountains has been drying for the last half of the century;
2. If the current climate is drying, then evaluate how much and whether the dryness was sufficient to result in dark-needled conifer forests decline and dieback at mid-to-higher elevations as referenced in recent literature [16]; and
3. If the predicted climate changes (AR5 [53] result in increased dry conditions, would these be sufficient to force a severe decline and/or dieback of the climax dark-needled forests by the end of the 21st century.

To achieve these goals, we investigated dryness/moisture indices and overall meteorological-ecosystem dynamics from 1961–2019 across the South Siberia Mountains and modeled dark-needled forest areas in a changing climate for the 1961–2019 period and for the 2080 s (2070–2100) using our Montane Bioclimatic vegetation model, MontBioCliM [54].

2. Data and Methods

2.1. Geographic Study Area

The mountains (Mts) of southern Siberia are located in the center of the Asian continent and stretch latitudinally for three-thousand kilometers. Their elevation reaches more than 3000 m a.s.l. The mountains act as barriers that intercept moisture-bearing air masses to create favorable conditions for growing shade-tolerant, water-loving tree species, Siberian pine (*Pinus sibirica* Du Tour) and Siberian fir (*Abies sibirica* Ledeb.). These shade-tolerant tree species are cataloged as dark-needled conifers in Russian geobotanic classifications. The mountains of southern Siberia are a unique geographical region characterized by diverse natural conditions that are comparable with West Siberia or Central Siberia.

The mountains serve as a watershed basin between the Arctic and Pacific oceans and the inland Central Asia basin. This location, which is distant from the oceans, determines both climate and vegetation over the study area. The South Siberian Mountains encompass the following mountain ranges: Altai, West and East Sayan, Salair-Kuznetsky Alatau, Mts of the Republic of Tyva, Pribaikalye (west of Lake Baikal), Transbaikalia (east of Lake Baikal), and the Stanovoi Range [55] within the geographic window between 49–56 °N and 82–114° E (Figure 1).

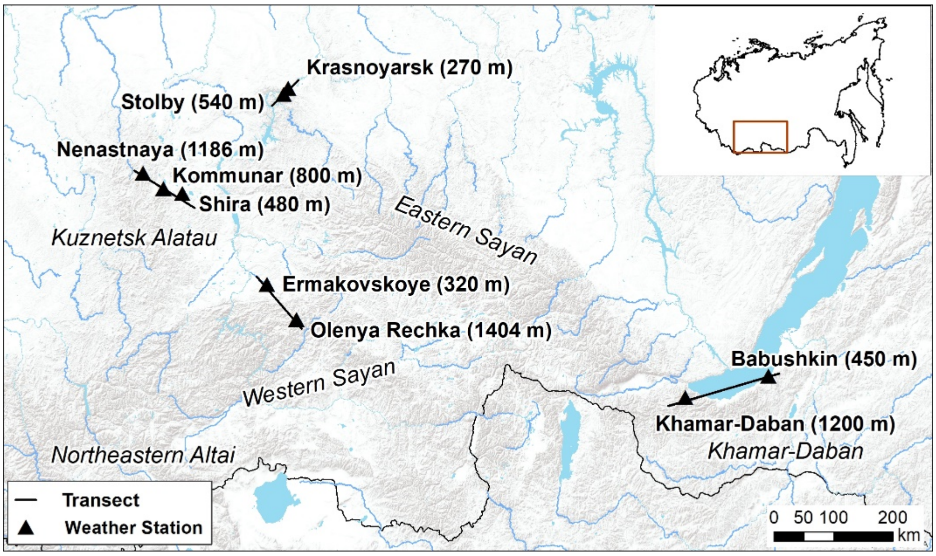

Figure 1. Four climate transects based on 9 weather stations located by pairs at low and high elevations: 1. Transbaikalia: st. Babushkin—st. Khamar-Daban; 2. Western Sayan: st. Ermakovskoye—st. Olenya Rechka; 3. Kuznetsky Alatau: st. Shira—st. Kommunar—st. Nenastnaya; 4. Eastern Sayan: st. Krasnoyarsk—st. Stolby. Dark blue is lakes (left to right): Uvs nuur; Hovsgol nuur; Baikal.

2.2. Vegetation and Climate

Vegetation. The South Siberian Mountains are known as lush, highly productive forests with a high degree of biodiversity. They are classified into three bioclimatic sectors: (1) West Siberia sector—moderate continentality and moisture, (2) East Siberia—high continentality and less moisture, and (3) inland Central Asia—high continentality and a subarid/arid climate [55].

The first sector, the Altai-Sayan mountains, is represented by the altitudinal belts (from low to high elevations): steppe, forest-steppe and subtaiga, 'chern', montane, and subalpine taiga. Chern translates to 'black' in Russian and represents lush, productive forests rich in flora, including some tertiary species and ferns. On windward slopes, 'chern' dark-coniferous forest dominate with tree species that include Siberian cedar (*Pinus sibirica*), Siberian fir (*Abies sibirica*), and spruce (*Picea obovata*). On leeward slopes, dominant tree species are Siberian larch (*Larix sibirica*) and pine (*Pinus sylvestris*).

The East Siberian sector is represented by East Sayan, Pribaikalye, and Transbaikalia; this sector is represented by the altitudinal belts: steppe, forest-steppe, and subtaiga (*P. sibirica, L. sibirica, and L. dahurica*), middle-elevation montane taiga, and the high-altitude *P. sibirica—L.* spp. taiga followed by a fragmented subalpine belt. The forest-belt structure of the near-Baikal range is composed of forest-steppe (segments of *P. sibirica*) and subtaiga (*P. sylvestris and L. sibirica*), 'chern' taiga (*A. sibirica*), middle-elevation taiga (*P. sibirica*, *A. sibirica*, and *L. sibirica)*, sporadic subalpine taiga (sparse stands of *P. sibirica and A. sibirica*), and subalpine tundra with fragments of dwarf *Pinus pumila* Rgl.

The Central Asia sector encompasses the southeastern Altai and southern Tyva, and this sector is composed of steppe, forest-steppe, tundra-steppe, and tundra altitudinal belts. The forests consist of *L. sibirica,* which are located only on northern-facing slopes in lowland pseudo-taiga, middle-elevation taiga, and highland subalpine altitudinal belts. This is a relatively dry region, so the increased solar radiation on the southern-facing slopes results in steppe landscapes, with strips of forest-steppe and forest on northern-facing and naturally sheltered areas.

Climate in Siberia is the most continental on Earth, a largely dry climate that experiences the largest temperature range on Earth. The South Siberian Mts region is located in inland Central Asia, where the climate is dominated by the extreme distance from oceans. The Atlantic Ocean plays the dominant role in transporting moisture across the continent to the region. The southern mountains act to intercept the precipitation that remains from the westerly flow from the Atlantic across Siberia, thus restricting precipitation across Siberia. The largest amount of precipitation falls in the north-western Altai highlands—1800 mm a year. In contrast, on the leeward range, in the intermontane southeast Altai basin, only 200–400 mm a year are reported. About 50% of annual precipitation falls in July and August. Snow cover is typically minimal (10–20 cm) in intermountain basins but increases upslope in the mountains, up to 2 m. The Siberian High results in low temperatures, especially in the intermountain basins: absolute minima in winter may reach correspondingly: −50 °C in Altai, −58 °C in Tyva, and −65 °C in Transbaikalia. High summer temperatures result from southern heat waves from Mongolia and northern China: 30 °C in Altai and Tyva and 35 °C in Transbaikalia [1].

Climate has been changing in montane southern Siberia in the last 60 years. Summers have become increasingly warmer (by 0.7–1.5 °C), and winters have become warmer by 1–2 °C in the farming regions of southern Siberia. For instance, both summer and winter temperatures have increased by 1.4–3.2 °C in the Minusinsk Hollow and by 2–4 °C in the southern farming regions in Tyva, close to the Mongolian border [3,56–58]. Patterns of precipitation are complicated by the complex topography across the southern mountains. In general, the climatic moisture trends based on weather station data have shown increased wetness in forests and increased dryness in steppe zones [59].

2.3. Climate Data

Long-term monthly mean January and July temperatures and annual precipitation prior to 1960 were collected from 280 weather stations (reference books on climate, 1967–1970) across the South Siberian Mountains. Most of these weather stations are located at lower elevations, and only 45 weather stations are located above 1000 m, and 3 of these are above 2000 m. In this study, climate data were extended (www.meteo.ru/data accessed on 27 July 2022) for nine weather stations to calculate current climate change trends from 1961 to 2019 (see below).

2.4. Montane Climate Models

For these models, climate data of January and July temperatures and annual precipitation from the 280 weather stations across the study region were used to interpolate to a 10 km resolution using Hutchinson's thin-plate smoothing splines ANUSPLIN (https://fennerschool.anu.edu.au/research/products/anusplin accessed on 27 July 2022). Thereafter, three bioclimatic indices were calculated using the weather station data (growing degree-days above 5 °C (GDD_5), negative degree-days below 0 °C (NDD), annual precipitation, and annual moisture index (AMI equal to a ratio between GDD_5 and annual precipitation)) to initialize our *Montane Bioclimatic Vegetation Model* (MontBioCliM) [54] for mapping the montane vegetation across the South Siberian Mountains for the analyzed timeframes (see details of MontBioCliM [54,55,60,61] in Supplementary 2).

2.5. Climate Change Trends

Historic climate change trends were constructed for the 1961–2019 period to capture potential climate change trends that could result in the decline and/or dieback of dark-needled forests along four transects over the last 60 years. Due to the scarcity of mountain stations, the following four pairs of stations at lower and upper elevations along these transects were used to calculate lapse rates of climatic variables:

- Stations Shira (458 m), Kommunar (842 m) and Nenastnaya (1186 m) in the Kuznetsky Alatau Mts;
- Stations Ermakovskoye (300 m) and Olenya Rechka (1404 m) in the Western Sayan Mts;
- Stations Krasnoyarsk (274 m) and Stolby (536 m) in the Eastern Sayan Mts; and
- Stations Babushkin (480 m) and Khamar-Daban (1442 m) in Transbaikalia Mts

Here, the station elevations above sea level (asl) are shown in parentheses.

2.6. Climate Change Scenarios

Future January and July temperatures and annual precipitation were calculated for each of 20 CMIP5 GCM projection (www.ipcc-data.org accessed on 27 July 2022) by summing anomalies relative to the contemporary climatic layers to produce the resultant 2080 s temperature and precipitation [58]. Thereafter, we conducted averaging of all patterns of each climate variable for 20 GCMs to obtain ensembles of mean anomalies. Finally, the ensemble means for 20 GCMs were calculated for two scenarios. The mild RCP 2.6 scenario and extreme RCP 8.5 scenario correspond to an overall radiative forcing by the year 2080 of 2.6 and 8.5 Wm^{-2}, respectively.

2.7. Standardized Precipitation Evapotranspiration Index (SPEI)

SPEI [62] was tested in this study to assess drought conditions over the South Siberian Mts. SPEI is a site-specific drought indicator of fluctuations around the average water balance. SPEI is calculated using a climatic water balance technique (P (precipitation)—PET (potential evapotranspiration)), which is the accumulation of a deficit or surplus at different time scales, adjusted to a log-logistic probability distribution (Supplementary 2. Figures S1 and S2). The SPEI is defined by five drought severity classes: SPEI > −0.5 no drought; −1 < SPEI < −0.5 light drought; −1.5 < SPEI < −1 moderate drought; −2 < SPEI < −1.5 severe drought and SPEI < −2 extreme drought [63].

Vicente-Serrano et al. [62] calculated PET using monthly temperatures at a variety of temporal periods (from three to twenty-four months). We compared PET calculated for twelve months using the Vincente-Serrano [62]) methodology to PET calculated by Budyko methodology [64] (Supplementary 1). PET calculated using the Budyko methodology was 15% larger than PET calculated using the Vicente-Serrano et al. methodology. Hereafter, we used SPEI calculated using the Vicente-Serrano methodology to be consistent with their results. Vicente-Serrano et al. [65] found the maximum SPEI to NDVI (Normalized Difference Vegetation Index) correlations in boreal ecosystems using twelve-month PET. Five- to six-month PET was found to correlate well between SPEI and tree-ring data.

The climate in montane regions is complicated by complex topography that includes rapid variations in elevation, slope, and aspect. We additionally evaluated PET on steep south-facing slopes to determine if droughts could occur in these dryer habitats. Polikarpov et al. [1] found PET was up to 25% greater on southern, southwest, and southeast than on flat surfaces and northern slopes (Supplementary 1. Table S1).

2.8. The Vitality/Health State of a Damaged Forest

First, we visited every Leskhoz (a forestry enterprise) or national reserve located in our four transects, and the chief forester reported information about the decline/dieback of dark-needled forests and showed us their locations. We examined several plots (2–5 plots, see for details Table 1) along each of our four transects. A complete enumeration of 150–200 trees on each plot (circa 0.25 ha) was carried out, and each tree was visually categorized into four health classes based on characteristic photosynthetic and generative apparatus damage: healthy (number of trees, n_1), damaged (n_2), severely damaged (n_3), dying and dead (n_4) trees. We followed the Alexeev approach [5] developed from his decades of forestry experience. Alexeev determined four health classes for trees: a healthy tree has a 100% vitality potential; a damaged tree has lost 1/3 of its vitality down to 70%; a severely damaged tree has 40% vitality left; and a dying tree has only 5% vitality remaining. He also developed an empirical formula for the health index (In, %) of a stand:

$$\text{In} = (100 \cdot n_1 + 70 \cdot n_2 + 40 \cdot n_3 + 5 \cdot n_4)/N \quad (1)$$

where N is the total number of trees in a stand including dead trees.

Finally, Alexeev defined four stand health classes: 1. Healthy, undamaged stands In ≥ 80%; 2. Damaged stands In = 50–79%; 3. Severely damaged stands In = 20–49%; 4. Dying and dead stands In < 20%.

The years with damage were reconstructed based on the Tretyakova and Bazhina method; see [26] for details. At each plot, 3–5 damaged trees that had been cut down or felled by windfall were selected for analyses (Table 1). The number of examined trees could reach 50–90 on special occasions (e.g., windfall). The crown elements of both healthy and damaged trees were measured: the extent of a tree crown, the distance between whorls, the number of branches in the whorls, the angle of a branch attachment to the tree, and the localization and extent of the damaged part of the crown (in both meters and in the number of whorls). Finally, the year of damage was associated with the whorl below which the damage was detected. Thus, the year of damage was reconstructed by counting years top-down starting from the year of tree felling.

Table 1. Locations of damaged dark-needled stands over the South Siberian Mountains. Years of damage (bold) matching years of SPEI<−1.5 (red) and SPEI>1.5 (blue) or preceding them.

<table>
<tr><th>Region, Stations</th><th>Elevation, m a.s.l.</th><th>Slope Aspect</th><th>Vitality Index</th><th>Years of Damage</th><th>Years of SPEI < −1.5 Severe Droughts</th><th>Years of SPEI > 1.5 Wet Years</th></tr>
<tr><td>Khamar-Daban Transect (bottom-up):
Babushkin –Khamar-Daban</td><td>H:1100–1190</td><td>SW, NW</td><td>55–64
Damaged</td><td>1960–1961
1968
1971–1973
1976–1977
1980–1983</td><td>1964
1986
1997–1999
2002
2017</td><td>1966
1969
1971
1973
1985
1988
1991
2008</td></tr>
<tr><td>Eastern Sayan, Transect leeward (bottom-up):
Krasnoyarsk –Stolby</td><td>M: 450–640
M: 680–820</td><td>River valleys
River and stream headwaters, watersheds</td><td>70
Damaged
58–68
Damaged</td><td>***1973–1974***
1978
1982–86
1991–93
1998–99</td><td>1962
1973
1997</td><td>1969
1972
1979
1987
1996
2013
2014</td></tr>
<tr><td rowspan="3">Western Sayan, Transect windward (bottom-up):
Ermakovskoe–Olenya Rechka</td><td>M: 800</td><td rowspan="2">Northern macroslope</td><td>36
Severely damaged</td><td rowspan="3">***1978–82***
1985–87
1989–90
1993–96
1999</td><td rowspan="4">***1989***
1999
2011</td><td rowspan="4">1972
1979
1980
1985
1987
1998
2006
2009</td></tr>
<tr><td>H: 1420–1450</td><td>55
Damaged</td></tr>
<tr><td>H: 1150–1500</td><td>Pass,
Axial part</td><td>80.0–81.5
Healthy</td></tr>
<tr><td>Western Sayan, Transect windward (Rock et al.1991)</td><td>M: 700–1000</td><td>West-facing slopes</td><td>Damaged</td><td>before-1990s</td></tr>
<tr><td>Kuznetsky Alatau, Transect windward (bottom-up):
Kommunar – Nenastnaya</td><td>M: 570–1000</td><td>SE, SW, NW</td><td>46.4–57.5
Severely damaged</td><td rowspan="2">1991
1999</td><td rowspan="2">1980–81
1989–90 1997
1999
2005
2011–12
2016</td><td rowspan="2">1964
1970
2002
2018</td></tr>
<tr><td>Transect leeward (bottom-up):
Shira-Kommunar</td><td>M: 710–1250</td><td>NW, SW</td><td>65.6–92.3
Damaged to healthy</td></tr>
</table>

Elevation: L—low; M—medium and H—high. Red indicates damage and drought years; blue indicates damage and wet years.

3. Results

3.1. Dieback of the Dark-Needled Forests Observed for the 1961–2019 Period

Our examination of damaged trees in dark-needled forests located across the South Siberian Mts showed that most dieback was found in the middle-elevation taiga at 700–900 m and partially in high elevation taiga at 1100–1200 m in all four mountain systems (Altai, Western and Eastern Sayans, and the southern Transbaikalia) before the Polygraphus beetle invasions occurred in the first decade of the 2000s (Table 1). Massive dieback was not detected in the most climatically favorable lowland chern taiga (300–500 m), highland subalpine taiga (1450–1500 m) in the Western Sayan Mts. and in the highland subalpine taiga (1800–2000 m) in the northeastern Altai Mts. A significant decline of the fir resistance was found only in some middle-elevation fir stands growing at 640–830 m over ridges of the Eastern Sayan Mts close to the city of Krasnoyarsk. It is worth noting that dark-needled forests growing at about the same elevations at 820–830 m on the Dzhebsky Pass in the Eastern Sayan Mts and at 880–1200 m on the Aradan and Oisky Ridges in the West Sayan Mts were found healthy and categorized 'undamaged'. In these systems, all damaged trees were old (older than 90 years old) and, as a rule, were found with the disease of rust fungi (*Melampsorella cerastii* Wint).

Most fir and Siberian pine trees were weakened to various degrees in stands started in the 1960s at highlands of 1100–1200 m on the Khamar-Daban Ridge in Transbaikalia; at elevations 800–1420 m on northern slopes of the Kulumys and Oisky Ridges in the Western Sayan; and at 710–1250 m on the ridges of Kuznetsky Alatau. Retrospective examinations of damaged fir tree canopies showed that dieback was found to move from the east to the west. The fir dieback started in the eastern part of the Khamar-Daban Ridge range, and massive dieback was associated with the 1976–1977 and 1980–1982 periods [19,26]. At middle elevations on ridges in the Eastern Sayan Mts., individual trees started to decline and die in 1973–1974, 1978, 1982–1985, 1991–1993, and 1998–1999 (Table 1).

On the northern macroslope of the Western Sayan Mts., the dieback of dark-needled conifer forests started later, and dieback waves were marked in 1978–1982, 1989, 1994–1996, and 1999 (Table 1). Massive dieback of *Abies sibirica* in the western part of its distribution over the South Siberian Mts. was found in 1991 and 1999 in Kuznetsky Alatau Mts. and in 2003–2004 in the northeastern Altai Mts.

Thus, several critical periods of synchronized massive *Abies sibirica* and *Pinus sibirica* decline were identified in the middle-to-high elevation mountain taiga across the South Siberian Mts in: 1978, 1980–1982, 1998–1999, 2003, and 2005.

3.2. Climate Change Time Series for 1961–2019

To correlate moisture dynamics for 1961–2019 with the decline of dark-needled forests across the South Siberian Mts, we used two moisture/dryness indices that relate to heat and water supply/demand: AMI and SPEI (see definitions above). Annual AMI and SPEI were well correlated (r = −0.49–0.84) with large correlation coefficients in dryer conditions (Supplementary 2. Figure S2). Note, the aridity degree increases with growing positive AMI and with decreasing negative SPEI.

In our bioclimatic models, we defined values of AMI limit distributions of terrestrial ecosystems at various scales: at the continental scale for Siberia [60,66] and at the regional scale for the Altai-Sayan Mts [54] that is a part of the South Siberian Mts. The critical values of AMI for the forest types were defined as follows: AMI = 3.5 as the border between the forest (mixed deciduous and light-needled conifer) and steppe; and AMI = 2.25 as the border between light-needled and dark-needled forests. We concentrated on the AMI dynamics at elevations where decline/dieback of dark-needled forests was identified in situ. The 60-year AMI dynamics for 1961–2019 were constructed for nine weather stations along four transects across the South Siberian Mts (Figure 2).

As follows from Figure 2, AMI did not reach the critical limit of 2.25 for 1961–2019 at stations located in the subalpine highlands (stations: Khamar-Daban, Olenya Rechka, and Nenastnaya) and middle-elevation dark-needled taiga (stations: Stolby and Kommunar).

AMI reached the limit of 2.25 only at low elevation dark-needled taiga (station Babushkin) starting in the 21st century. Even at forest-steppe stations Krasnoyarsk and Ermakovskoye, the AMI crossed the critical value of 3.5 occasionally during the 60-year period eight and two times, respectively. Only at the steppe station Shira, AMI values were predominantly above 3.5 and were below 3.5 (moist) only 4 times for 60 years. Thus, the AMI dynamics do not indicate evident tendencies of climate aridization in the dark-needled forests across the South Siberian Mts.

SPEI was applied to our study area across the South Siberian Mts by Kharuk et al. et seq. [16] to provide evidence that the decline and mortality of dark-needled forests have been induced by the drying climate. We demonstrate using one transect (stations: Shira-Kommunar-Nenastnaya in the Kuznetsky Alatau Mts, (Figure 3) that for the 1961–2019 period, the negative water balance ((P-PET) ≤ 0, that characterized droughts) occurred only at weather station Shira located in the steppe zone. At stations Kommunar (842 m a.s.l.) and Nenastnaya (1186 m a.s.l.), between which the dark-needled forest was located, the annual water balance was always positive during the 1961–2019 period. However, SPEI at these three stations varied within the same values (Figure 4).

In addition to the AMI dynamics, SPEI dynamics were calculated to identify severe and extreme drought conditions during 1961–2019. SPEI time series were calculated for the same nine weather stations located by pairs at low-to-high elevations along four elevation transects (Figure 5). Our findings showed that climatic drought indices rarely went down to high risk levels during the last 60 years (1961–2019). These levels are characterized by SPEI < -1.5 values and are representative of drought stress conditions of dark-needled conifers dieback/survival. Drought conditions at stations with SPEI < -1.5 occurred 3–4 times and occurred only 1–2 times in two sequential years with SPEI < -1.5 during the 60-year period.

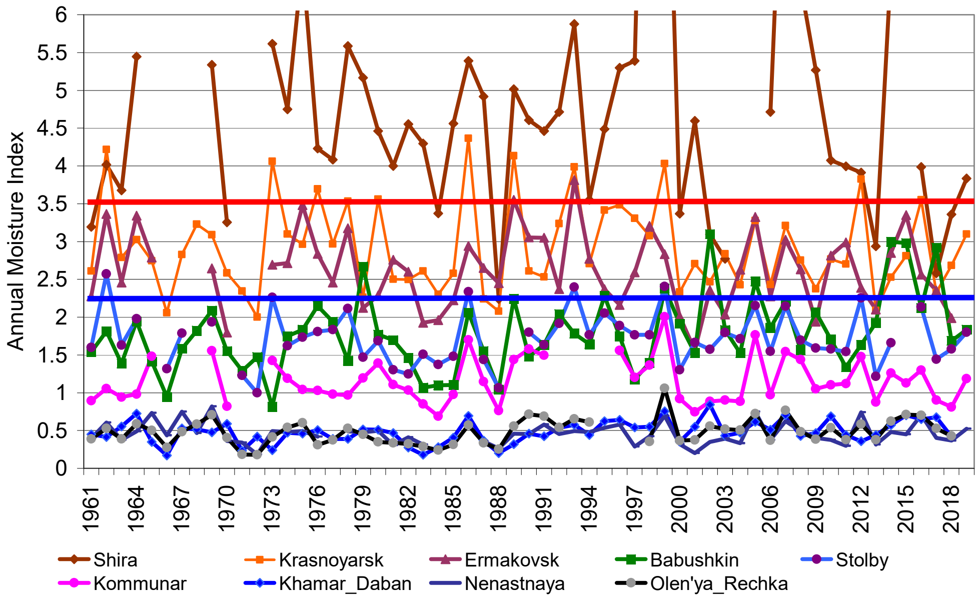

Figure 2. The AMI time series for 1961–2019 at nine weather stations across the South Siberian Mountains, in the east-west direction: 1. Highland subalpine dark-needled taiga: stations Khamar-Daban, Olenya Rechka, and Nenastnaya; 2. Middle-elevation dark-needled taiga: stations Babushkin, Stolby, Kommunar; 3. Subtaiga-forest-steppe: stations Krasnoyarsk and Ermakovskoye; and 4. Steppe: station Shira. The red line (AMI = 3.35) is the border between forest and steppe, and the blue line (AMI = 2.25) is the border between light-needled and dark-needled forests.

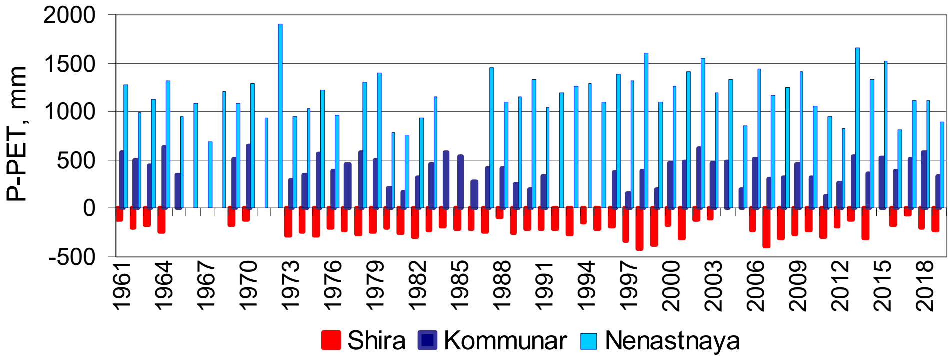

Figure 3. Water balance (P–PET) at three weather stations located along a 50-km transect in various landscapes in the Kuznetsky Alatau Mts: st. Shira at 468 m a.s.l.—Steppe, st. Kommunar at 870 m a.s.l.—Dark-needled taiga, and st. Nenastnaya at 1186 m a.s.l.—Subalpine dark-needled taiga.

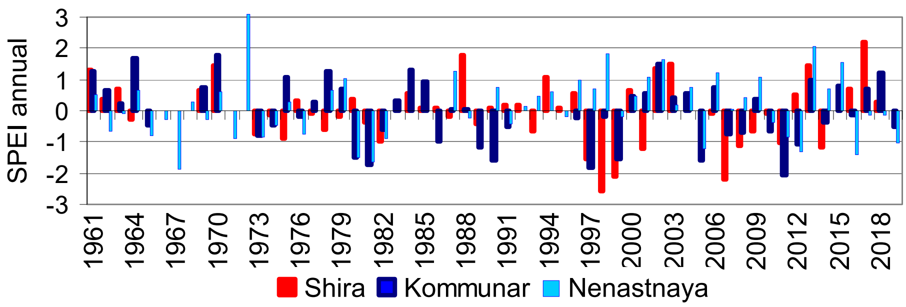

Figure 4. Annual SPEI time series for three different vegetation types in the Kuznetsky Alatau Mts: st. Shira at 468 m a.s.l.—Steppe, st. Kommunar at 870 m a.s.l.—Dark taiga, and st. Nenastnaya at 1186 m a.s.l.—Subalpine dark taiga.

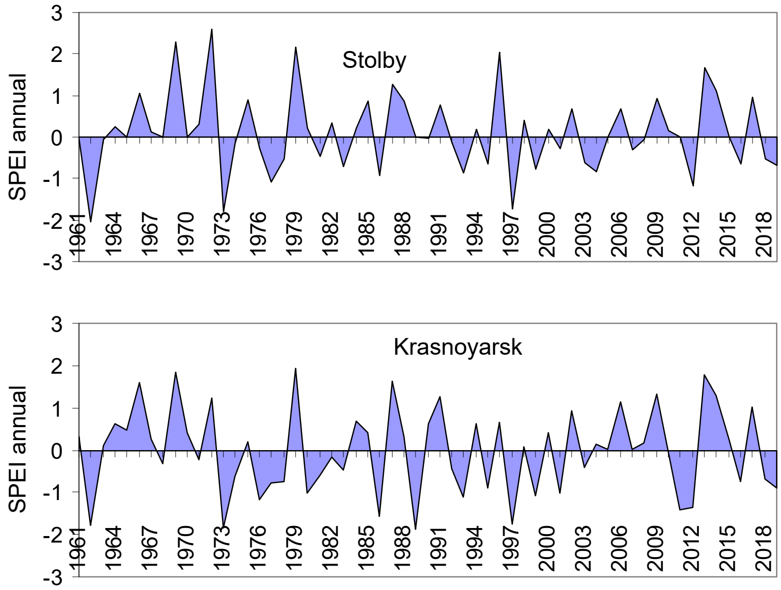

(**a**)

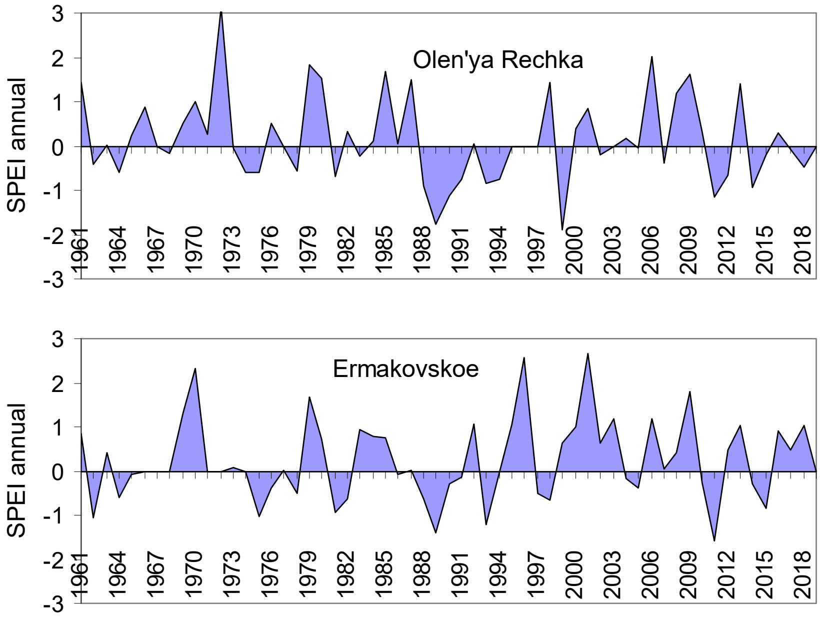

(**b**)

Figure 5. *Cont*.

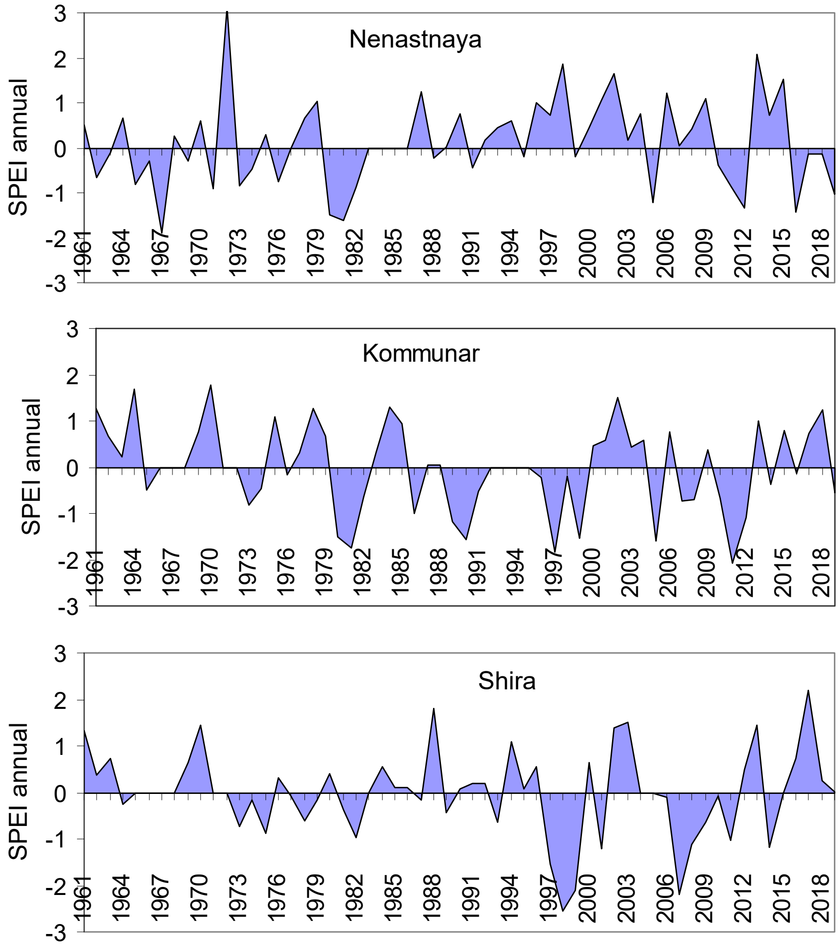

(**c**)

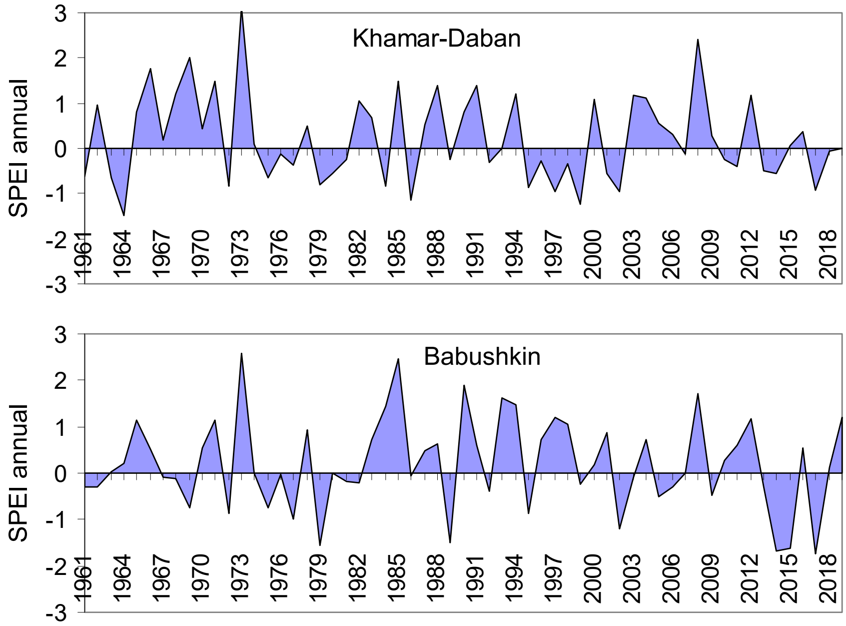

(**d**)

Figure 5. SPEI time series for 1961–2020 along elevation transects in Eastern Sayan (**a**), Western Sayan (**b**), Kuznetsky Alatau (**c**), and Khamar-Daban (**d**) Mts. Legend. Years in black are of extreme droughts by SPEI of <−1.5 across mountain ranges. Years in red are matches between severe canopy

damage and extreme droughts by SPEI; years in blue are matches between severe canopy damage and extreme moisture. (**a**) **Eastern Sayan transect: sts.** Stolby (536 m a.s.l.)—Krasnoyarsk (274 m a.s.l.). SPEI: Extreme droughts: 1962, **1973**, **1997**; Extreme moisture: 1969, **1972**, 1979, **1996**; Severe canopy damage: **1973**–1974, 1978, 1982–86, 1991–93, **1998–1999**. (**b**) **The Western Sayan transect: sts.** Olen'ya Rechka (1404 m a.s.l.)—Ermakovskoye (300 m a.s.l.). SPEI: Extreme droughts: **1989, 1999**; Extreme moisture: 1974, **1979–1980, 1985–1987**, 2006, 2009; Severe canopy damage: **1978–1982**, **1985–1987**, **1989–1990**, 1993–1996, **1999** (no data available after 2000). (**c**) **The Kuznetsky Alatau transect: sts.** Nenastnaya (1186 m a.s.l.)—Kommunar (842 m a.s.l.)—Shira (458 m a.s.l.). SPEI: Extreme droughts: 1980–1981, 1990, 1997, **1999**, 2005, 2011; Extreme moisture: 1964, 1970; Severe canopy damage: 1991, **1999** (no data available after 2000). (**d**) The Khamar-Daban transect: sts. Khamar-Daban (1442 m a.s.l.)—Babushkin (480 m a.s.l.). SPEI: Extreme droughts: 1964; Extreme moisture: 1966, 1969, **1973**, 2008; Severe canopy damage: 1960–1961, 1968, 1971–1973, 1976–1977, 1980–1983.

We carried out additional quantitative analyses (see Supplementary 3). We grouped all SPEI data for 1960-2000 for three highland stations (Khamar-Daban, Olenya Rechka, and Stolby), which were close to damaged plots (differences in elevation between these stations and sites were 50-200 m) and assigned a damage degree, D, equal to 1 "damage was observed" to 0 "no-damage was observed" for each year. Applying t-test for these data, we determined that mean SPEI values for damage/no-damage years did not significantly differ for current year as well as for three previous years (Supplementary 3: Tables S1 and S2; Figure S1).

4. Discussion

Vicente-Serrano et al. [65] stated: " … wet and moist forests of each ecoregion are always located in areas with a positive water balance, where the control of vegetation activity by drought is low, as indicated by low correlation with the SPEI. In cold regions, where temperature, instead of precipitation, is the major constraint on plant development, there is little influence of drought on vegetation activity, resulting in low correlations too." This statement is confirmed by our findings across the South Siberian Mts (Supplementary 2. Figure S2) that in cold and wet dark-needled forests at mid-to-high elevations, characterized by high rain and thus low AMI, there was a low correlation between SPEI and AMI. A high correlation between SPEI and AMI was found in warm and dry subtaiga forests, which are transitioning to steppes, where Vicente-Serrano et al. [65] stated that "dry biomes in temperate, subtropical, and tropical regions show the highest correlations with the SPEI."

SPEI was defined by Vicente-Serrano et al. [62] as a drought index applied to dry Mediterranean forest ecosystems with limited moisture, often causing water stress. Trees evolved specific defense mechanisms, such as the sclerophyllous leaves that have a waxy outer layer ('hard leave' in Greek) to limit transpiration under water stress in hot and dry Mediterranean summers. Across the boreal zone with sufficient moisture, SPEI values below -1.5 may not be evidence of insufficient moisture if the water balance remains positive, as in the case in northerly forests or at higher elevations over mountains in the temperate and boreal zone. However, in many studies, SPEI is used as a drought index in moist temperate and boreal forests. As a measure of the climatic water balance variations (the accumulation of deficit/surplus water at different time scales) with emphasis on negative SPEI values below -1.5, it is important to know how often these events occur and would the water balance remains positive for trees to survive.

It is known from forestry textbooks that trees are capable of recovering two dry sequential years [67]. Vicente-Serrano et al. [65] emphasized that trees survive occasional droughts characterized by annual SPEI values of <-1.5. Usually, trees could not recover after sequential 3–4 drought years [18]. We did not see steady aridization trends indicating a drying climate at middle-to-high elevations over the South Siberian Mts. that could cause the dieback of dark-needled forests. The SPEI values < -1.5 that are characteristic of extreme droughts occurred only 3–4 times during the 1961–2019 period. Trees are known to recover successfully after 1 to 2 years of drought.

Statements about droughts using only SPEI criteria not accompanied by the water balance values seems to be not climatically sound for sufficiently moist forests characterized by a positive water balance on a 6-month to 12-month basis. Our earlier study in the South Siberian Mts [1] showed that dark-needled forests are located in moist conditions that are characterized by an annual water balance of (P − PET) > 100 mm on leeward macroslopes to 300 mm over watersheds to 600 mm on windward macroslopes. For instance, in the Kuznetsky Alatau Mts., both stations, Nenastnaya (subalpine woodland) and Kommunar (dark-needled taiga), satisfied this moisture condition of a positive annual water balance, but station Shira (steppe) did not (Figure 3). However, SPEI at all three stations varied within the same limits, predominantly $\pm$ 1.5 (Figure 4). Even though SPEI values dropped down to −2.1 in 2011 at the dark-needled taiga st. Kommunar, the annual water balance remained substantially positive (> 150 mm per year; Figure 3).

SPEI is commonly calculated for various periods: 1, 3, 6, 12, and 18 months, depending on study goals. It is logical to use 1–3-month summer SPEI to evaluate drought risks for yearly agriculture crops. However, using 1–3-month SPEI to provide reasons for forest ecosystems' dieback without taking into consideration accumulated winter water is not convincing. Our detailed eddy-covariance study in a Scots pine forest in Central Siberia showed that trees survived two monthly May–June droughts with a negative water balance for three sequential years [68] (Supplementary 2, Table S1).

In their studies, Kharuk et al. [16] used SPEI data that have been gridded globally with 0.5 by 0.5 degrees of resolution for the period starting from 1901. Using such gridded data over extensive plain terrains is fair. However, over mountain terrains where several biomes (steppe, forest, tundra) may occur in one cell of 50 by 50 km and be characterized by one station usually located in mountain foothills, using such gridded data to correlate with field plots of the linear size of 10–20 m is quite questionable.

Large global low-resolution data sets (0.5 degree SPEI) are not suitable for characterizing critical ecosystems that exist at a portion of that scale, especially over complex terrain where micrometeorological effects are significant, and biomes change abruptly due to orographic effects.

Field examinations along four transects showed that tree damage occurred at mid-to-higher elevations between 800 and 1200 m on windward montane macroslopes. Climate data for 1961–2019 demonstrated that moisture conditions at these sites have not changed much and were sufficient to support dark-needled forests. Taking into account that the AMI limit for the lower/southern border of dark-needled forests is 2.25, the AMI variations between 0.8 and 0.2 at 800–1200 m elevations indicate very wet conditions. Modeled moisture conditions for dark conifers would still remain satisfactory at the 2080s for both the moderate RCP 2.6 and even extreme scenario RCP 8.5 (Supplementary 2. Figures S4 and S5). Extreme droughts characterized by the SPEI <−1.5 occurred occasionally, only 3–4 times during the historic 1961–2019 period, during which the dark-needled forests could be capable of surviving.

Kharuk et al. [16] found a decline in the number and health of the dark-needled conifer trees on the southern slopes at their low limits in the Eastern Sayan and Kuznetsky Alatau. Our calculations showed that PET increased up to 1.25-fold on the southern-facing steep slopes [1] (Supplementary 1. Table S1). However, the water balance ($P - PET_{slope}$) stayed essentially positive (Supplementary 2, Figure S2) even for the lower limits of dark-needled conifers at station Kommunar (842 m a.s.l., Kuznetsky Alatau). Only at station Stolby (542 m a.s.l., East Sayan) was the annual water balance negative (−100 mm) on occasional years separated by a decade or two: 1962, 1973, and 1997. As said above, the dark-needled conifers would be capable of surviving after one-year dry conditions.

We support another hypothesis. Dark-needled conifer dieback across the South Siberian Mts often occurs in the wet years with plentiful rain rather than in the drought years (Table 1).

On the windward transect in the Khamar-Daban Ridge, the years of damage 1971–1973 concurred with the wet years 1971 and 1973. On the windward transect in the Western

Sayan Mts, 1979, 1985, and 1987 were wet, and these years also showed significant forest damage. This phenomenon had been described as far back as the end of the 19th century. Scientists found that damage in trees depended on the water amount in the polluted air: damage was greater if carried out by pollution brought by wet air masses rather than by dry air masses [69].

In Kuznetsky Alatau, along the leeward transect with less precipitation, our observations were conducted in the decade 1991–1999. Only one year of damage in 1999 matched the dry 1999.

A double combination of a wet year followed by a dry year resulted in heavy damage to trees. In the Eastern Sayan, the damage in 1973–1974 was preceded by the combination of the wet year of 1972 followed by the dry year of 1973; and the damage in 1998–1999 was preceded by the combination of the wet year of 1996 followed by the dry year of 1997. In West Sayan, the damage occurred in 1999 after the wet year in 1998, followed by a dry year in 1999.

We relate the phenomenon of dark-needled conifer dieback in the South Siberian Mts. to the westerlies that bring rain from the Atlantic to interior Asian Russia. The air masses of the westerlies come from the west, collecting atmospheric pollution across most of the populated regions along the 50–58 N latitudes, which are full of industries. The South Siberian Mts are the barriers on the way of the westerlies that force the most polluted rain (acid rain) to precipitate at mid-to-higher elevations along the windward northwestern slopes [1]. The danger of forest dieback grows with an increase in the rain with elevation increases and the high susceptibility of dark-needled conifers, especially Siberian fir, to acid rain [1,70]. Rehfuess [6] noted the significance of pollutants and acidic deposition, as one cause (among others), for Norway spruce decline at higher elevations in Germany.

Sulfur dioxide, a major acid rain impurity, is a potent poison for the photosynthetic apparatus (leaves). It damages leaf cell membranes causing the leaf transpiration rate to increase several-fold, which decreases the total water content, chemically bound water, and the water retention capacity of leaves resulting in tree top-drying [69].

Recent results of the 11-year monitoring of acid impurities in the atmosphere in the southern Lake Baikal regions showed tendencies of the steady increase in acids in rains that are under the impact of large industrial centers. Acid rains are the greatest threat to natural objects (forests, water, etc.) in these southern regions, in particular, the windward slopes of the Khamar-Daban Range, which are on the path of the polluted air masses from regional industrial plants across southern Siberia [71,72].

5. Conclusions

Field examinations of dark-needled forests across the South Siberian Mountains show that most of the severely damaged vegetation is located at middle and higher elevations between 800 and 1200 m on windward montane slopes. Climate observations from 1960 to 2019 show that moisture conditions did not change enough to result in severely damaged vegetation; thus, changes in the moisture balance do not support the climate-induced aridization hypothesis. The annual moisture index calculated for weather stations located at these elevations varied between 0.2 and 0.8 on average, which indicated very wet conditions. The AMI limit for the dark conifers is 2.25. Even in the future, in a drying climate by the end of the 21st century, including the most severe climate change scenarios, moisture conditions would remain quite satisfactory for dark-needled conifer *Pinus sibirica* and *Abies sibirica* stands.

We conclude that the grounds for the observed decline in dark-needled conifers at the middle-to-high elevations across the South Siberian Mts includes a complex of causes, of which a dryer climate does not show the strongest relationship, as cited in recent literature. Plausible causes that trigged the decline/dieback of dark-needled conifer forests in the South Siberian should be additionally investigated.

Literature searches and this research show that air pollution combined with precipitation strongly impacts leaf metabolism damaging photosynthetic apparatus. However, literature and the SPEI show the relationship to precipitation could be much more complicated than originally imagined, so an abundance of precipitation could affect leaf physiology that results in delayed leaf damage, ~2-years after the 'abundance' event, when combined with substantial air pollution. Future research should be extended based on regular observations of air chemistry associated with meteorological conditions in damaged forest sites. Data of this kind are limited and often not accessible. This research has led us to conclude that the effects, processes, and mechanisms involved in the complex interactions between pollution, precipitation, and the combined impact on tree physiology and dieback are worthy of extended interdisciplinary research. Results are essential for understanding these ecosystems and others as our planet changes. This research would necessitate creating an infrastructure that supports teamwork between forestry, plant physiology, and atmospheric physics/chemistry institutions, organized under governmental and business support.

Supplementary Materials: The following supporting information can be downloaded at: https://www.mdpi.com/article/10.3390/f13091378/s1, Supplementary 1: Table S1: The ratio between evapotranspiration on slope to flat surface; Supplementary 2: Figure S1: Water balance (P –PET, mm) time series on a flat surface (upper) and on a steep south-facing slope 20-30 degree (lower) at the lower limit of the dark-needled forests in Kuznetsky Alatau (at st. Kommunar, 842 m, blue) and Eastern Sayan (at st. Stolby, 536 m, orange); Figure S2: The dependence of the correlation coefficients between SPEI and AMI on annual precipitation; Figure S3: Vegetation types modeled across the South Siberian Mountains using the MontBioClim: 1–Tundra; 2–Subalpine woodland; 3–Dark-needled taiga; 4–Light-needled taiga; 5–Subtaiga and Forest-steppe; 6–"Chern" (Black) taiga; 7–Steppe; 8–Dry Steppe/Semidesert. Blue circles are nine weather stations used in our analyses: 1–Babushkin; 2–Khamar-Daban; 3–Ermakovskoe; 4–Olen'ya Rechka; 5–Shira; 6–Kommunar; 7–Nenastnaya; 8–Krasnoyarsk; 9-Stolby., Figure S4: The dark-needled taiga ranges (blue) across the South Siberian Mountains: in the baseline climate (upper), in the RCP 2.6 2080 climate (middle), and transition hot spots of dark-needled forest to steppe (orange) and tundra to dark-needle (green); no change is grey. Red points are 9 weather stations; Figure S5: The dark-needled taiga ranges (blue) across the South Siberian Mountains: in the RCP 8.5 2080 climate (upper), and transition hot spots of dark-needled taiga to forest-steppe (orange) and tundra to dark-needled taiga (green); no change is grey. Red points are 9 weather stations: Table S1: Monthly water balance in a pine forest (Tchebakova et al. 2002).; Supplementary 3: Figure S1: S. Annual (left) and 3-summer month (right) mean SPEI values for damaged (1) and no-damaged (0) dark-needled forest stands for three meteostations located close to the damaged stands. Stations: STLB–Stolby, OR–Olenya Rechka, KD–Khamar-Daban., Table S1: Results of the SPI difference assessment of the "damage" and "no damage" occurrence years at three highland stations (Khamar-Daban, Olenya Rechka, and Stolby) using the Student t-test. Assessment was conducted for annual SPEI values for current and three preceding years. The t-values that are less than 2 by absolute value indicate that for years with damage and without damage the SPEI differences are statistically insignificant at the 0.05 level., Table S2: Results of the SPI difference assessment of the "damage" and "no damage" occurrence summers at three highland stations (Khamar-Daban, Olenya Rechka, and Stolby) using the Student t-test. Assessment was conducted for June-July-August SPEI values for current and three preceding years. The t-values that are less than 2 by absolute value indicate that for years with damage and without damage the SPEI differences are statistically insignificant at the 0.05 level.

Author Contributions: Conceptualization, N.M.T. and E.I.P.; methodology, N.M.T., E.I.P. and E.V.B.; validation, N.M.T. and E.V.B.; formal analysis, E.I.P.; investigation, E.V.B. and E.I.P.; resources, E.V.B. and E.I.P.; writing—original draft preparation, N.M.T.; writing—review and editing, N.M.T., A.J.S., E.I.P., E.V.B. and P.Y.G.; visualization, E.I.P. and A.J.S.; funding acquisition, N.M.T. All authors have read and agreed to the published version of the manuscript.

Funding: This research received no external funding.

Institutional Review Board Statement: Not applicable.

Informed Consent Statement: Not applicable.

Data Availability Statement: www.meteo.ru (accessed on 27 July 2022).

Acknowledgments: N.M.T., E.I.P., and E.V.B. acknowledge the support from the Russian Foundation for Basic Research, project #20-05-00540 acknowledge and N.M.T. acknowledges climate data provided by National Park Krasnoyasrk Stolby. The work of P.Y.G is supported by the NSF grant no. 2020404 'Belmont Forum Collaborative Research: Coastal OceAn SusTainability in Changing Climate' and no. 2127343 'NNA Collaborative Research: Frozen Commons: Change, Resilience and Sustainability in the Arctic'. The authors are heartily grateful to our dear friend Jane Bradford for English editing.

Conflicts of Interest: The authors declare no conflict of interest.

References

1. Polikarpov, N.P.; Tchebakova, N.M.; Nazimova, D.I. *Climate and Montane Forests of Southern Siberia*; Nauka: Novosibirsk, Russia, 1986; p. 226.
2. Semechkin, I.V.; Polikarpov, N.P.; Iroshnikov, A.I.; Babintseva, R.M.; Vorob'ev, V.N.; Dashko, N.V.; Ivanov, V.V.; Kondakov Yu, P.; Korotkov, I.A.; Murina, T.K.; et al. *Pinus Sibirica Forests of Siberia*; Nauka: Novosibirsk, Russia, 1985; p. 258.
3. Tchebakova, N.M.; Parfenova, E.I.; Korets, M.A.; Conard, S. Potential change in forest types and stand heights in central Siberia in a warming climate. *Environ. Res. Lett.* **2016**, *11*, 35016. [CrossRef]
4. Groisman, P.; Bulygina, O.; Henebry, G.; Speranskaya, N.; Shiklomanov, A.; Chen, Y.; Tchebakova, N.; Parfenova, E.; Tilinina, N.; Zolina, O.; et al. Dryland belt of Northern Eurasia: Contemporary environmental changes and their consequences. *Environ. Res. Lett.* **2018**, *13*, 115008. [CrossRef]
5. Alekseev, V.A. Diagnostics of tree vitality and stand condition. *Lesovedenie* **1989**, *4*, 51–57.
6. Rehfuess, K. Review of forest decline research activities and results in the federal republic of Germany∗. *J. Environ. Sci. Health Part A* **1991**, *26*, 415–445. [CrossRef]
7. Huettl, R.F.; Mueller-Dombois, D. (Eds.) *Forest Decline in the Atlantic and Pacific Region*; Springer: Berlin, Germany, 1995; p. 366. [CrossRef]
8. Manko, Y.I.; Gladkova, G.A.; Butovets, G.N.; Kamibayashi, N. Monitoring of fir-spruce forests dieback in the Central Sikhote-Alin. *Lesovedenie* **1998**, *1*, 3–15.
9. Manko, Y.I.; Gladkova, G.A. *Spruce Decline in the Light of Global Deterioration of Dark Coniferous Forests*; Dal'nauka: Vladivostok, Russia, 2001; p. 228. (In Russian)
10. Contreras-Hermosilla, A. The Underlying Causes of Forest Decline. CIFOR. Oc. Paper No. 30. 2000; p. 29. Available online: https://www.cifor.org/publications/pdf_files/OccPapers/OP-030.pdf (accessed on 27 July 2022).
11. Johnstone, J.F.; Chapin, F.S. Fire Interval Effects on Successional Trajectory in Boreal Forests of Northwest Canada. *Ecosystems* **2006**, *9*, 268–277. Available online: https://www.jstor.org/stable/25470335 (accessed on 27 July 2022). [CrossRef]
12. Allen, C.D.; Macalady, A.K.; Chenchouni, H.; Bachelet, D.; McDowell, N.; Vennetier, M.; Kitzberger, T.; Rigling, A.; Breshears, D.D.; Hogg, E.H.; et al. A global overview of drought and heat-induced tree mortality reveals emerging climate change risks for forests. *For. Ecol. Manag.* **2010**, *259*, 660–684. [CrossRef]
13. Lindenmayer, D.B.; Laurance, W.F.; Franklin, J.F. Global Decline in Large Old Trees. *Science* **2012**, *338*, 1305–1306. [CrossRef]
14. Kharuk, V.I.; Im, S.T.; Oskorbin, P.A.; Petrov, I.A.; Ranson, K.J. Siberian pine decline and mortality in Southern Siberian mountains. *For. Ecol. Manag.* **2013**, *310*, 312–320. [CrossRef]
15. Kharuk, V.I.; Im, S.T.; Petrov, I.A.; Golyukov, A.S.; Ranson, K.J.; Yagunov, M.N. Climate-induced mortality of Siberian pine and fir in the Lake Baikal Watershed, Siberia. *For. Ecol. Manag.* **2017**, *384*, 191–199. [CrossRef]
16. Kharuk, V.I.; Im, S.T.; Petrov, I.A.; Dvinskaya, M.L.; Shushpanov, A.S.; Golyukov, A.S. Climate-driven conifer mortality in Siberia. *Glob. Ecol. Biogeogr.* **2020**, *30*, 543–556. [CrossRef]
17. Saigin, I.A.; Bartalev, S.A.; Stytsenko, F.V. 2019 Detecting method of long-term dieback of dark-needled forests of Russia on the base of remote sensing data. In Proceedings of the 17th All-Russia Open Conference "Modern Problems of the Earth Remote Sensing", Moscow, Russia, 11–15 November 2019; p. 445. Available online: http://conf.rse.geosmis.ru/files/pdf/17/7902_IKI_konf2019_3(2)(1)__1.pdf (accessed on 27 July 2022).
18. DeSoto, L.; Cailleret, M.; Sterck, F.; Jansen, S.; Kramer, K.; Robert, E.M.R.; Aakala, T.; Amoroso, M.M.; Bigler, C.; Camarero, J.J.; et al. Low growth resilience to drought is related to future mortality risk in trees. *Nat. Commun.* **2020**, *11*, 1–9. [CrossRef]
19. Bazhina, E.V. Seed production and quality in Abies sibirica Ledeb. in zone exposed to influence of the Baikal Pulpaner Factory. *Russ. J. For. Sci.* **1998**, *2*, 10–15.
20. Bazhina, E.V. Siberian fir (Abies sibirica) state and chemical element allocation in tree crown in forest ecosystems of Protected Areas in south of Krasnoyarsk Region (Russia). *Nat. Conserv. Res.* **2018**, *3*, 40–53. [CrossRef]
21. Bazhina, E.V. Living status of Siberian fir (Abies sibirica Ledeb.) and element composition of its needle in the Middle Siberia Mountain forest ecosystems. *Reg. Ecologia* **2018**, *2*, 7–16. [CrossRef]
22. Bazhina, E.V.; Tretyakova, I.N. Towards a problem of Fir decline. *Uspekhi Sovrem. Biologii.* **2001**, *121*, 626–631.
23. Bazhina, E.V.; Aminev, P.I. Peculiarities of seed productivity and shoot morphology of fir trees affected by Melampsorella cerastii Wint. *Lesn. Zhurnal* **2007**, *3*, 7–13. (In Russian)

24. Bazhina, E.V.; Storozhev, V.P.; Tretyakova, I.N. Dieback of Fir-Siberian Stone pine forests under technogenic pollution in the Kuznetsky Alatau Mountains. *Lesovedenie* **2013**, *2*, 15–21.
25. Fedorov, N.I.; Sarnatsky, V.V. *Features of Creation of Spruce Forests of Belarus in Connectionwith Their Periodic Mass Drying*; Tekhnalogiya: Minsk, Belarus, 2001; 180p.
26. Tretyakova, I.N.; Bazhina, E.V. Structure of crown as well as pollen and seed viability of fir (Abies sibiica Ledeb.) in disturbed forest ecosystems of the Khamar-Daban Mts. *Ecology* **2000**, *19*, 280–294.
27. Tretyakova, I.N.; Bazhina, E.V.; Pakhar'kova, N.V.; Storozhev, V.N. The state of fir-pine stands on territory of Natural Park "Ergaki" and their fluorescent diagnostics. *Conifers Boreal Area.* **2008**, *XXV*, 237–243.
28. Voronin, V.I.; Morozova, T.I.; Stavnikov, D.Y.; Nechesov, I.A.; Oskolkov, V.A.; Buyantuyev, V.A.; Mikhaylov, Y.Z.; Govorin, Y.V.; Seredkin, A.D.; Shuvarkov, M.A. Bacterial Damage of Cedar Forests of the Baikal Region. *Lesn. Khozaistvo* **2013**, *3*, 39–41.
29. Voronin VI, Sofronov AP, Morozova TI, Oskolkov VA, Sukhovol'skii VG, Kovalev AV 2019 The landscape-specific occurrence of bacterial diseases in dark-coniferous forests on Khamar-Daban range (Southern Cisbaikalia). *Geogr. Nat. Resour.* **2019**, *4*, 56–65. [CrossRef]
30. Shiyatov, S.G.; Terent'ev, M.M.; Fomin, V.V.; Zimmermann, N.E. Altitudinal and horizontal shifts of the upper boundaries of open and closed forests in the Polar Urals in the 20th century. *Rus. J. Ecol.* **2007**, *38*, 223–227. [CrossRef]
31. Theurillat, J.P.; Guisan, A. Potential impact of climate change on vegetation in the European Alps: A review. *Clim. Change* **2001**, *50*, 77–109. [CrossRef]
32. Belova, N.A.; Morozova, T.I. Dynamics of forest pathology condition of fir stands of the Baikal Nature Reserve (1983–2015). *For. Bull.* **2018**, *22*, 5–15.
33. Donaubauer, E. On the Decline of Fir (Abies densa Griff.) in Bhutan. In *Forest Decline in the Atlantic and Pacific Region*; Huettl, R.F., Mueller-Dombois, D., Eds.; Springer: Berlin, Germany, 1993; pp. 332–339. [CrossRef]
34. Pavlov, I.N. Biotic and abiotic factors as causes of coniferous forests dieback in Siberia. *Far East Contemp. Probl. Ecol.* **2015**, *22*, 537–554. [CrossRef]
35. *Forest Decline and Air Pollution: A Study of Spruce (Picea, Abies) on Acid Soils*; Schulze, D.E.B. (Ed.) Springer: Berlin/Heidelberg, Germany; New York, NY, USA; London, UK; Paris, France, 1989; Volume 78, 475p.
36. CARB 2021 New analysis shows spikes of metal contaminants, including lead. In *2018 Camp Fire Wildfire Smoke*; California Air Resources Board: Sacramento, CA, USA. Available online: https://ww2.arb.ca.gov/news/new-analysis-shows-spikes-metal-contaminants-including-lead-2018-camp-fire-wildfire-smoke (accessed on 25 January 2022).
37. Kristensen, L.J.; Taylor, M.P. Fields and Forests in Flames: Lead and Mercury Emissions from Wildfire Pyrogenic Activity. *Environ. Health Perspect.* **2012**, *120*, a56–a57. [CrossRef]
38. Turetsky, M.R.; Harden, J.W.; Friedli, H.R.; Flannigan, M.; Payne, N.; Crock, J.; Radke, L. Wildfires threaten mercury stocks in northern soils. *Geophys. Res. Lett.* **2006**, *33*, L16403. [CrossRef]
39. Gaitnieks, T.; Klavina, D.; Muiznieks, I.; Pennanen, T.; Velmala, S.; Vasaitis, R.; Menkis, A. Impact of Heterobasidion root-rot on fine root morphology and associated fungi in Picea abies stands on peat soils. *Mycorrhiza* **2016**, *26*, 465–473. [CrossRef]
40. Pavlov, I.N.; Barabanova, O.A.; Ageev, A.A. Resistance Reduction of Fir-Cedar Forests of Eastern Sayan Mountains to Root Pathogens. *IVUZ Lesn. Zhurnal* **2011**, *4*, 40–45. Available online: http://lesnoizhurnal.ru/apxiv/2011/%E2%84%964-2011.pdf (accessed on 27 July 2022).
41. Pavlov, I.N.; Litovka, Y.A.; Golubev, D.V.; Astapenko, S.A.; Chromogin, P.V.; Usoltseva, Y.V.; Makolova, P.V.; Petrenko, S.M. Mass reproduction of Polygraphus proximus Blandford in fir forests of Siberia infected with root and stem pathogens: Monitoring, patterns, biological control. *Contemp. Probl. Ecol.* **2020**, *13*, 71–84. [CrossRef]
42. Krivets, S.A.; Bisirova, E.M.; Kerchev, I.A.; Pats, E.N.; Chernova, N.A. Transformation of taiga ecosystems in the Western Siberian invasion focus of four-eyed fir bark beetle Polygraphus Proximus Blandford (Coleoptera: Curculionidae, Scolytinae) *Russ. J. Biol. Invasions* **2015**, *6*, 94–108. [CrossRef]
43. Kerchev, I.A.; Mandelshtam, M.Y.; Krivets, S.A.; Ilinsky, Y.Y. Small spruce bark beetle Ips amitinus (Eichhoff, 1872) (Coleoptera, Curculionidae: Scolytinae): A new alien species in Western Siberia. *Entomol. Rev.* **2019**, *99*, 639–644. [CrossRef]
44. *Forest Decline and Ozone. A Comparison of Controlled Chamber and Field Experiments*; Sandermann, H.; Wellburn, A.R.; Heath, R.L. (Eds.) Ecological Studies, Analysis and Synthesis; Springer: Berlin, Germany, 1997; Volume 127, p. 390. [CrossRef]
45. Stanhill, G.; Cohen, S. Global dimming: A review of the evidence for a widespread and significant reduction in global radiation with discussion of its probable causes and possible agricultural consequences. *Agric. For. Meteorol.* **2001**, *107*, 255–278. [CrossRef]
46. Wild, M. Global dimming and brightening: A review. *J. Geophys. Res. Atmos.* **2009**, *114*, D00D162009. [CrossRef]
47. Sicard, P.; Anav, A.; De Marco, A.; Paoletti, E. Projected global ground-level ozone impacts on vegetation under different emission and climate scenarios *Atmos. Chem. Phys.* **2017**, *17*, 12177–12196. [CrossRef]
48. Zuev, V.V.; Zueva, N.E.; Korotkova, E.M.; Pavlinsky, A.V. The impact of ozone depletion to degradation processes of coniferous forests in the southern regions of Siberia. *Atmos. Ocean. Opt. J.* **2017**, *30*, 342–348. [CrossRef]
49. Matyushevskaya, E.V. Factors of Variability of Tree Radial Increment. 2017, p. 231. Available online: https://elib.bsu.by/handle/123456789/190614 (accessed on 27 July 2022). (In Russian).
50. Mills, G.; Pleijel, H.; Malley, C.S.; Sinha, B.; Cooper, O.R.; Schultz, M.G.; Neufeld, H.S.; Simpson, D.; Sharps, K.; Feng, Z.; et al. Tropospheric Ozone Assessment Report: Present-day tropospheric ozone distribution and trends relevant to vegetation. *Elementa: Sci. Anthr.* **2018**, *6*, 47. [CrossRef]

51. Feng, Z.; De Marco, A.; Anav, A.; Gualtieri, M.; Sicard, P.; Tian, H.; Fornasier, F.; Tao, F.; Guo, A.; Paoletti, E. Economic losses due to ozone impacts on human health, forest productivity and crop yield across China. *Environ. Int.* **2019**, *131*, 104966. [CrossRef]
52. Kirdyanov, A.V.; Krusic, P.J.; Shishov, V.V.; Vaganov, E.A.; Fertikov, A.I.; Myglan, V.S.; Barinov, V.V.; Browse, J.; Esper, J.; Ilyin, V.A.; et al. Ecological and conceptual consequences of Arctic pollution. *Ecol. Lett.* **2020**, *23*, 1827–1837. [CrossRef]
53. IPCC. Contribution of Working Groups I, II and III to the Fifth Assessment Report of the Intergovernmental Panel on Climate Change. In *Climate Change 2014: Synthesis Report*; Core Writing Team, Pachauri, R.K., Meyer, L.A., Eds.; IPCC: Geneva, Switzerland, 2014; p. 151.
54. Tchebakova, N.M.; Parfenova, E.I.; Soja, A.J. The effects of climate, permafrost and fire on vegetation change in Siberia in a changing climate. *Environ. Res. Lett.* **2009**, *4*, 045013. [CrossRef]
55. Smagin, V.N.; Il'inskaya, S.A.; Nazimova, D.I.; Novosel'tseva, I.F.; Cherednikova, Y.S. *Forest Types of the Mountains in Southern Siberia*; Nauka: Novosibirsk, Russia, 1980; p. 336.
56. Soja, A.J.; Tchebakova, N.M.; French, N.H.; Flannigan, M.D.; Shugart, H.H.; Stocks, B.J.; Sukhinin, A.I.; Parfenova, E.I.; Chapin, F.S., III.; Stackhouse, P.W., Jr. Climate-induced boreal forest change: Predictions versus current observations. *Glob. Planet. Change* **2007**, *56*, 274–296. [CrossRef]
57. Tchebakova, N.M.; Parfenova, E.I.; Soja, A.J. Climate change and climate-induced hot spots in forest shifts in central Siberia at the turn of the 21st century *Reg. Environ. Change* **2011**, *11*, 817–827. [CrossRef]
58. Parfenova, E.; Tchebakova, N.; Soja, A. Assessing landscape potential for human sustainability and 'attractiveness' across Asian Russia in a warmer 21st century. *Environ. Res. Lett.* **2019**, *14*, 065004. [CrossRef]
59. Tchebakova, N.M.; Parfenova, E.I.; Lysanova, G.I.; Soja, A.J. Agroclimatic potential across central Siberia in an altered twenty-first century. *Environ. Res. Lett.* **2011**, *6*, 045207. [CrossRef]
60. Tchebakova, N.M.; Blyakharchuk, T.A.; Soja, A.J. Reconstruction and prediction of climate and vegetation change in the Holocene in the Altai–Sayan Mountains, Central Asia. *Environ. Res. Lett.* **2009**, *4*, 045025. [CrossRef]
61. Samoylova, G.S. Landscape Map of the Altai-Sayan Mountains. 2001; WWF-IGEM.
62. Vicente-Serrano, S.M.; Beguería, S.; López-Moreno, J.I. A Multiscalar Drought Index Sensitive to Global Warming: The Standardized Precipitation Evapotranspiration Index. *J. Clim.* **2010**, *23*, 1696–1718. [CrossRef]
63. Wang, Z.; Lyu, L.; Liu, W.; Liang, H.; Huang, J.; Zhang, Q.-B. Topographic patterns of forest decline as detected from tree rings and NDVI. *CATENA* **2020**, *198*, 105011. [CrossRef]
64. Budyko, M.I. *Climate and Life*; Academic Press: New York, NY, USA, 1974; p. 509.
65. Vicente-Serrano, S.M.; Gouveia, C.; Camarero, J.J.; Beguería, S.; Trigo, R.; Lopez-Moreno, J.I.; Azorin-Molina, C.; Pasho, E.; Lorenzo-Lacruz, J.; Revuelto, J.; et al. Response of vegetation to drought time-scales across global land biomes. *Proc. Natl. Acad. Sci. USA* **2013**, *110*, 52–57. [CrossRef]
66. Tchebakova, N.M.; Monserud, R.A.; Leemans, R.; Golovanov, S. A global vegetation model-based on the climatological approach of Budyko. *J. Biogeogr.* **1993**, *20*, 129–144. [CrossRef]
67. Kramer, P.J.; Kozlowski, T.T. *Physiology of Trees*; McGraw-Hill Book Company: New York, NY, USA, 1960.
68. Tchebakova, N.M.; Kolle, O.; Zolotoukhine, D.; Arneth, A.; Styles, J.M.; Vygodskaya, N.N.; Schluze, E.D.; Shibistova, O.; Lloyd, J. Inter-annual and seasonal variations of energy and water vapour fluxes above a Pinus sylvestris forest in the Siberian middle taiga *Tellus Ser. B Chem. Phys. Meteorol.* **2002**, *54*, 537–551. [CrossRef]
69. Bortitz, S.; Dassler, H.-G. *Einfluss von Luftverunreinigungen auf die Vegetation*; VEB Gustav Fischer Verlag Jena: Jena, Germany, 1976; 189p.
70. Rock, B.N.; Williams, D.L.; Kharuk, V.I.; Wessman, C.A.; Moss, D.M. Morphological, anatomical, and chemical characteristics of needle and branch samples of Siberian fir (Abies sibirica). In *Proceeding of the IGARSS'92 International Geoscience and Remote Sensing Symposium*; Houston, TX, USA, 26–29 May 1992, IEEE: Piscataway, NJ, USA, 1992; pp. 1289–1291. [CrossRef]
71. Belozertseva, I.A.; Vorobyeva, I.B.; Vlasova, N.V.; Yanchuk, M.S.; Lopatina, D.N. Chemical composition of snow in the water area of lake Baikal and on the adjacent territory. *Geogr. Nat. Resour.* **2017**, *1*, 90–99. [CrossRef]
72. Obolkin, V.A.; Netsvetaeva, O.G.; Golobokova, L.P.; Potemkin, V.L.; Zimnik, E.A.; Filippova, U.G.; Khodzher, T.V. The long-term results of acid fallout monitoring for the area of South Baikal. *Geogr. Nat. Resour.* **2013**, *2*, 66–73.